



An Optimised Design for the Linac4 Drift Tube Linac

S. Ramberger, P. Bourquin, Y. Cuvet, G. De Michele, F. Gerigk, J.-M. Giguet,
A.M. Lombardi, E. Sargsyan, M. Vretenar

CERN, Geneva, Switzerland

Abstract

For the new Linac4 injector at CERN, a Drift Tube Linac (DTL) has been designed for the energy range from 3 MeV to 50 MeV. This HIPPI note summarises the RF design, describes the mechanical structure and reviews the results achieved on prototype structures at the end of this HIPPI task.

Introduction

The design and optimisation of the CERN Linac4 Drift Tube Linac (DTL) has been undertaken within the HIPPI framework. The aim of the HIPPI work-package 2 concerning the DTL was to develop a design with respect to beam-dynamics, electro-magnetic and mechanic requirements and to test the design in a prototype. It has to be taken into account that the DTL design at CERN has Linac4 as an application in mind and thus the RF behaviour and the alignment mechanism were to be verified in order to make sure that a design developed in the HIPPI framework would be feasible for real accelerating structures.

As is typical for design work of some complexity, the design of the DTL evolved in iterations:

- An RF design was developed which would fulfil the basic requirements in acceleration from 3 MeV to 40 MeV with a low number of structures and a limited length based on beam physics requests.
- Beam dynamics calculations verified the critical beam parameters and adjusted the synchronous phase at each cavity in order to match the beam between RF structures and showing their feasibility.
- A prototyping phase was launched with international contributors going beyond the HIPPI framework and starting a first mechanical design phase.
- In parallel, a redesign was started to reduce known general issues of DTL structures and to adapt the design to new project parameters.
- As the production of the first prototypes did not progress as expected a second prototyping phase was launched at CERN. The mechanical design was completely reviewed and follows a new strategy which is discussed in this report.
- The parameters of the RF design were adapted following an overall optimisation of the linear accelerator with respect to the choice of RF structures. The new energy range became 3 MeV to 50 MeV following a comparison between the DTL and CCDTL shunt impedances, and due to refined assumptions on the output power from klystrons available at the cavities (1 MW in pulsed mode instead of the previously assumed 850 kW), a higher accelerating gradient could be chosen. This new design is the current RF design that is further discussed in this report.
- Beam dynamics simulations verified the feasibility of the new design.
- Meanwhile a prototype drift tube was received from the first prototyping cooperation and tested at CERN.
- With a full set of prototype drawings for the new prototype, the machining of parts was launched with outside contributors and the required assembly procedures were developed.
- The prototype was assembled at CERN and underwent low power RF tests and it is currently being prepared for high power tests. The results of these measurements are put in relation to the design values.
- Following mechanical design and prototype tests, a final re-iteration of the RF design and the beam dynamics will take place to find the DTL design to be built.

DTL working principle

Drift tube linacs generally consist in a cylindrical cavity with a number of drift tubes typically in the order of 30 suspended by stems for positioning along the beam axis. The resonator cavity is tuned to the required operating frequency with a field distribution of a TM₀₁₀ mode, i.e. a longitudinal electric field providing for the acceleration of particles on the beam axis in resonance with a circular magnetic field.

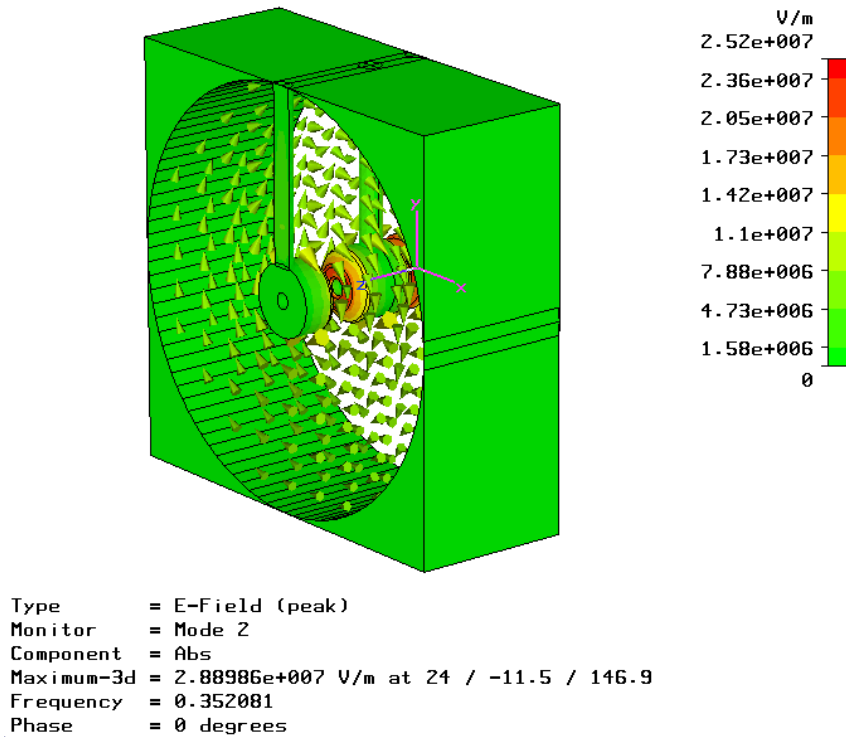


Figure 1: 3d simulation of one cell of a DTL with magnetic fields (arrows).

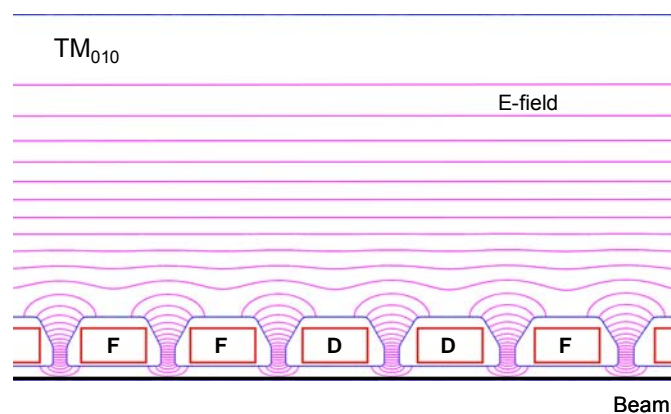


Figure 2: 2d simulation of DTL (longitudinal upper half x-section) with electric field lines.

During every period of the resonating electro-magnetic field, the particles proceed from one gap to the next such that they see a maximum electric field and thus accelerate each time when they are in the gap between drift tubes, and no electric field of the opposite sign while they are inside the drift tube. In order to achieve this condition, the length of the DTL cell has

to be $\beta \cdot \lambda$ with β the relativistic velocity coefficient and λ the wave-length of the resonating field. Magnets within the drift tubes indicated by F and D in figure 2 provide the transversal forces to keep the beam of particles focussed within the beam tube.

Geometrical description

The electro-magnetic design of a DTL cell is done with the program Superfish provided by Los Alamos National Laboratory, USA. In particular the special tuning code DTLfish provided with the Superfish program defines the geometry of the DTL cell using few key geometrical parameters as shown in figures 3 and 4 [1].

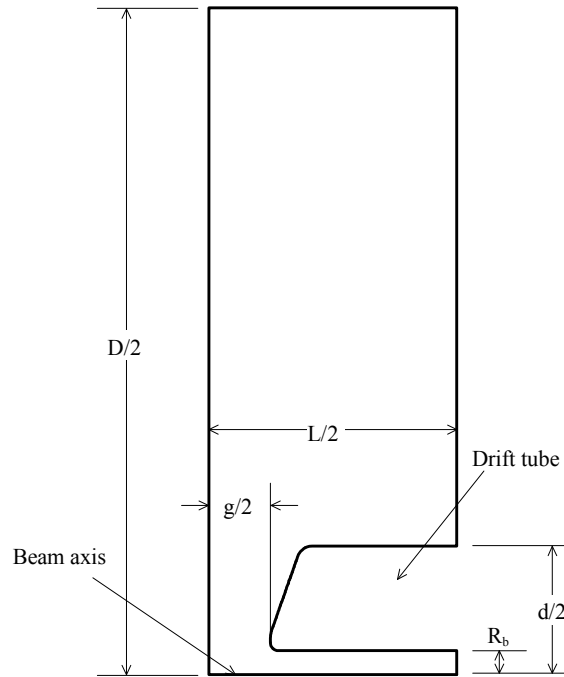


Figure 3: 3d simulation of one cell of a DTL with magnetic fields (arrows).

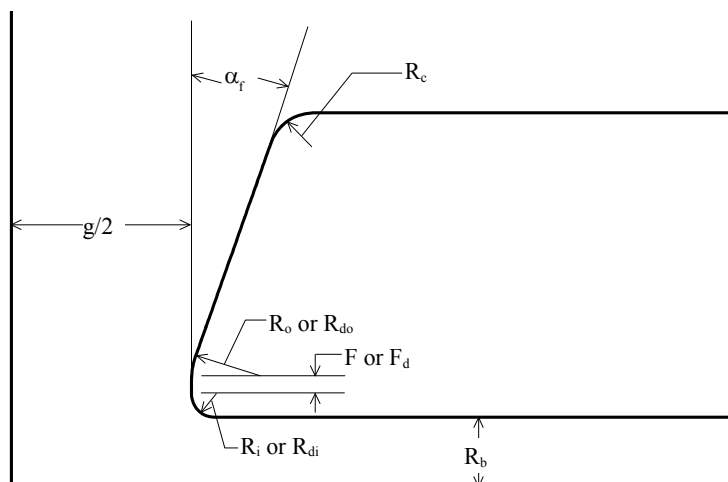


Figure 4: 3d simulation of one cell of a DTL with magnetic fields (arrows).

The resonance frequency is usually defined before the design of the accelerating structure starts. It is found considering availability of power sources and overall costs of the structures

General DTL Design

The Linac4 DTL shall accelerate H-ion beams of up to 40 mA average pulse current from 3 MeV to more than 40 MeV. While the input energy could be defined from experience early on, the exact output energy has to be found as a compromise between the DTL and the following accelerator stage, the Linac4 CCDTL [3]. The operating frequency was defined to 352.2 MHz in order to be able to reuse existing klystron power sources from the earlier LEP accelerator at CERN. A maximum duty cycle of up to 10% for Super Proton Linac (SPL) operation was defined in order to provide the required beam intensities for later upgrades.

A major decision to be taken early in the design is the magnet type: Traditionally electro-magnetic quadrupoles (EMQs) have been used inside the drift tubes for beam focusing. Alternatively quadrupoles made from permanent magnetic material can be used with the advantage of smaller size at medium magnetic gradients and the fact that no current supply wires or power converters are required.

The small size of permanent magnetic quadrupoles (PMQs) allows for a reduction in drift tube size with the advantage of lower effective shunt impedance per unit length, a measure for the effectiveness of acceleration. Beam dynamics define the size of the inner drift tube aperture. Following several design iterations, an optimum was found with 520 mm in cavity diameter with drift tubes of 90 mm diameter and 20 mm beam aperture. Each drift tube is equipped with a PMQ with an FFDD lattice in cavity 1 and an FD lattice in cavity 2 and 3. To ease matching for beam currents below nominal, electro-magnetic quadrupoles are placed in each of the inter-tank sections.

The choice of accelerating field E_0 is a compromise between the maximum reachable fields E_{max} , the available power and the acceleration to be achieved. It is important to note that the acceleration is proportional to the electric field whereas the losses are proportional to its square. This in turn means that at lower fields, longer tanks can be powered with the same output power from the klystron, making the acceleration more efficient. Longer tanks would thus be favourable if it wasn't for beam dynamics and manufacturing costs that call for shorter structures with higher gradients.

An additional limitation is the fact that maximum input power for cavities is available in discrete quantities only as defined by the number of klystrons. It is thus important to find a feasible and cost effective compromise: 5 klystrons that could be recuperated from the earlier LEP accelerator at CERN supplying 3 cavities, with 1 klystron on cavity 1, and 2 on each of cavity 2 and 3 was shown to lead to acceleration from 3 MeV to 40 MeV. Following a re-evaluation of the available output power from klystrons and the aim of reaching 50 MeV the E_0 was reduced to 3.2 MV/m, extending the overall length of the DTL tanks by 14%. Seen in the broader context of the full Linac4 accelerator, this modification was found to be advantageous as it can virtually save one klystron in the Linac4 and reduce operating costs.

E_0	W_{out}	Length	Klystron power
3.3 / 3.5 MV/m	40.1 MeV	2.6 / 5.2 / 5.2 m	0.8 MW
3.5 MV/m	47.7 MeV	2.9 / 6.3 / 6.4 m	1.0 MW
3.2 MV/m	50.6 MeV	3.5 / 7.4 / 7.3 m	1.0 MW

Table 1: Higher klystron power and lower E_0 result in higher output energy.

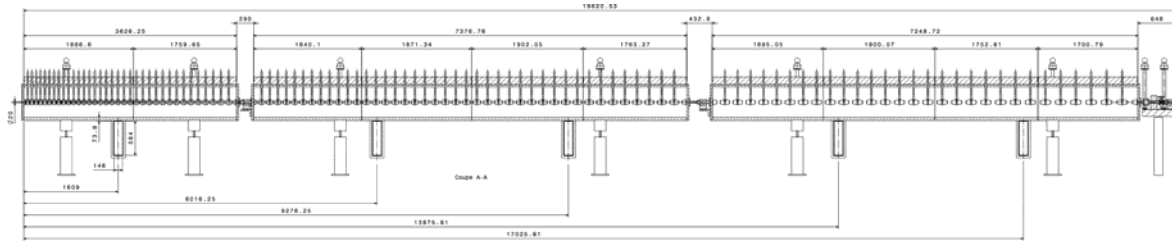


Figure 6: Linac4 DTL layout with 3 cavities.

Electro-Magnetic Design

Using experience from earlier iterations and beam dynamics calculations, the electro-magnetic design aims at acceleration with high constant average field E_0 over all gaps with high effective shunt impedance per unit length ZT^2 . While it is a typical DTL concept to ramp E_0 in the first cavity in order to adiabatically capture the beam longitudinally [4], the choice of high constant E_0 aims at maximizing the energy acceptance to the incoming beam and leads to a more compact design [5].

A particular advantage of ramping E_0 in the first cavity is lower peak fields at lower beam energies where earlier designs showed increased breakdowns [6]. Several parameters might be of influence: comparably large surfaces of flat opposing faces on consecutive drift tubes, more outgassing due to larger overall surfaces including the cavity end-wall, an incoming beam with a higher number of stray particles, magnetic fields close to surfaces of shorter drift tubes.

Recent studies for muon cooling where strong accelerating and magnetic fields have to be combined, emphasise the importance of the latter [7]. The PMQs that will be used for the DTL design have a peak magnetic surface field of 0.5 T which in the shortest drift tubes falls close to the area of peak electric fields.

In order to reduce breakdown probability in the first cells, the peak electric field therefore has been reduced by 30% by increasing the gap length. The cells are tuned by the face angle. At longer drift tubes the peak electric field can be ramped to values that allow for optimum effective shunt impedance (Fig. 7). In this way, the same advantage of lower peak fields in the first cells is achieved as when ramping E_0 without considerable decreasing the particle acceleration (E_0T).

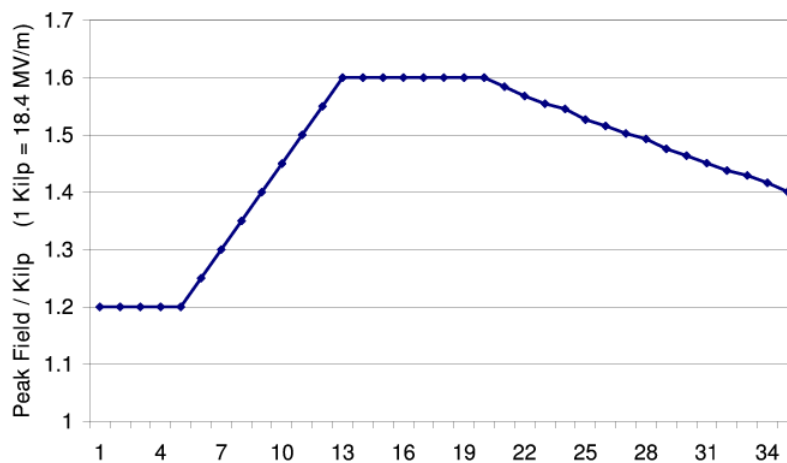


Figure 7: The peak electric field in the first cells was reduced to avoid breakdown.

The minimum gap length increases by 40% from about 8.5 mm to 11.9 mm. As a further advantage, also longitudinal mechanical tolerances increase by the same relative amount. The consequences on the effectiveness of the structure remain low. Energy gain in the first cells decreases by 4.1% but only 1% in beam energy over the first cavity is lost. The overall design reaches a beam output power of 50.1 MeV.

The overall DTL length is 18.7 m with the cavity parameters as shown in table 2:

Parameter	Cavity 1 / 2 / 3
Cells per cavity	36 / 42 / 30
Maximum surface field	1.6 / 1.4 / 1.3 Kilp
Synchronous phase	-30 to -20 / -20 / -20 deg
RF peak power per cavity	0.95 / 1.92 / 1.85 MW
RF beam / peak power	1.88 MW / 4.7 MW
Focusing scheme	FFDD / FD / FD
Quadrupole length	45 / 80 / 80 mm
Number of sections	2 / 4 / 4
Length per cavity	3.63 / 7.38 / 7.25 m

Table 2: Fundamental cavity parameters of the Linac4 DTL

2D RF Simulation Results

As mentioned earlier, 2D simulations have been done using the GEN_DTL program in conjunction with the Superfish 2D FEM program. Based on the general design parameters and starting from the input energy of 3 MeV, the DTL has been simulated cell by cell to find a self-consistent RF design that provides for maximum acceleration. Detailed cell-by-cell data are shown in the appendix; a summary is presented in table 3.

	Kilp	T _{avg}	E _{stored}	P _{Cu}	P _{beam}	P _{tot}	Effic.	E _{avg}	E _{gain}	Len	Z _s TT _{av}
Tank 1	1.60	0.85	11.043	588.87	360.60	949.47	0.380	0.258	9.015	361.84	45.24
Tank 2	1.39	0.89	22.817	1127.99	790.04	1918.03	0.412	0.470	19.751	741.70	53.29
Tank 3	1.27	0.84	22.521	1113.27	739.32	1852.60	0.399	0.616	18.483	728.17	48.11

Table 3: Cavity parameters of a self-consistent RF design for the Linac4 DTL

Power values are scaled up by 0.8, to account for additional losses with respect to simulations (e.g. post-couplers, tuners, RF port, RF contacts and surface roughness). Losses from stems and end-walls are included. ZTT values are scaled consistently with 0.8.

3D RF Simulation Results

In order to assess the effect of features that deviate from the main cylinder symmetry of the DTL, 3D simulations have been undertaken. In particular the effect of tuners, stems, post-couplers, and the wave-guide coupler require some attention. Cylindrical features like stems and post-couplers are usually accounted for by perturbation calculations on the basis of 2D simulations. 3D simulations confirm the results with higher accuracy. The dimensioning of the wave-guide coupler is of particular importance and can only be done accurately by 3D simulations.

Tuners

The effect of tuners can be estimated in 3D calculations (Microwave Studio) or as a perturbation effect of a 2D simulation (Superfish). Both simulations give about the same result: For a tuner of 90 mm diameter and 50 mm penetration, a frequency shift of 0.35 MHz·m and a loss of 2.5 kW (CW, scaled up by 0.8) is found.

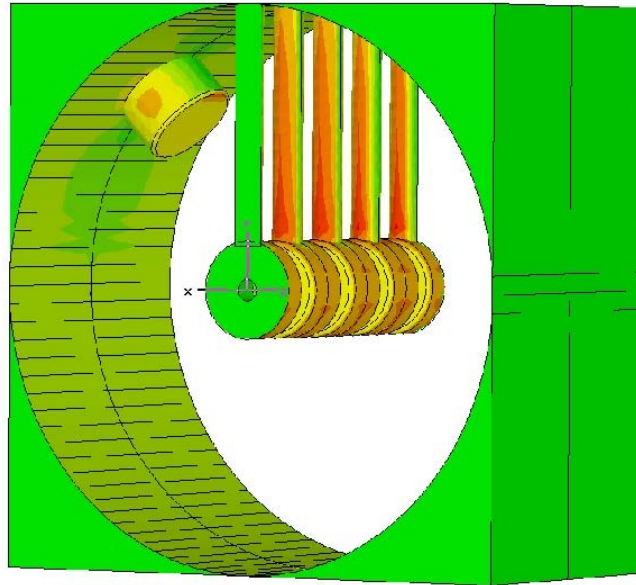


Figure 8: Surface currents on a small DTL structure with tuner.

Post-Couplers & Stabilization

The optimum nominal post-coupler length for minimum tilt sensitivity has been found in 3D simulations to be 174 mm. In figure 6, a main result of the study is reported showing the stabilising effect of post-couplers as measured by the tilt sensitivity with one post-coupler on every third drift tube as defined for the first cavity. The detailed results of this study can be found in the HIPPI publication [8].

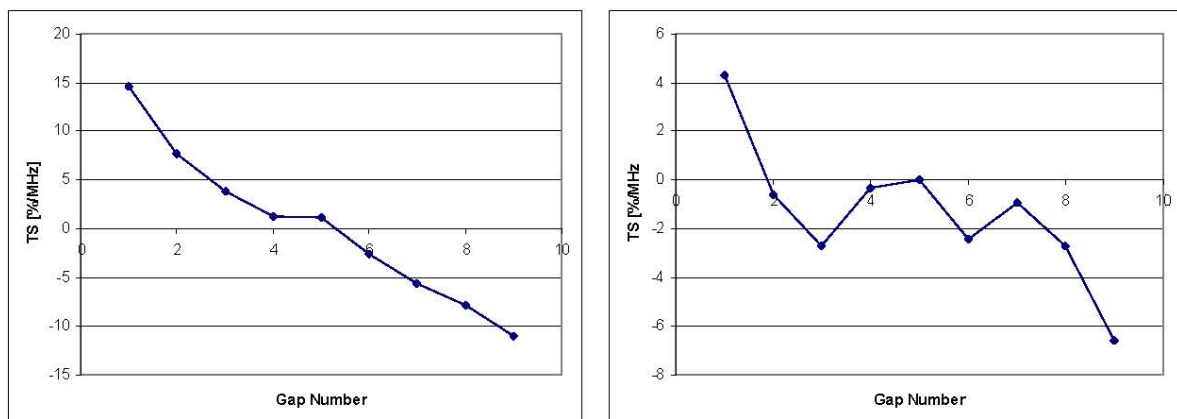


Figure 9: Simulation of the tilt sensitivity before and after stabilization.

Wave-guide coupler

In order to feed the RF power from the klystrons to a cavity, a system of standard wave-guides (type WR2300 in Linac4) and a coupler from the wave-guides to the resonator cavity is required. The design and dimensioning of an RF wave-guide coupler has been subject of a separate HIPPI task. The RF design for a 1 MW wave-guide coupler has been undertaken at CEA, Saclay and is reported in [9].

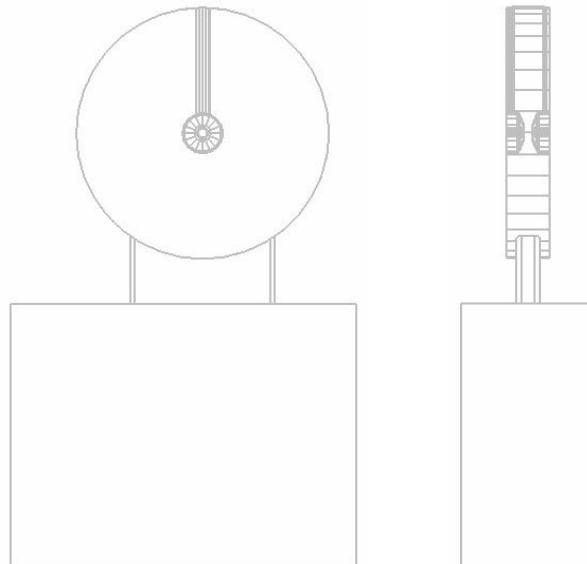


Figure 10: DTL wave-guide coupler: the RF envelope

This design represents a feasible solution for the Linac4 DTL. RF losses have been estimated, and the cooling design and manufacturing has been done by LPSC, Grenoble [10]. The final result is reported in [11].

Mechanical Design

The DTL cavities consist of a steel cavity, an aluminium girder, drift tubes assembled from pre-machined copper pieces, and accessories for mounting drift tubes in girders as well as for tuning, stabilization, support, vacuum pumping and alignment of the structures (Fig. 11).

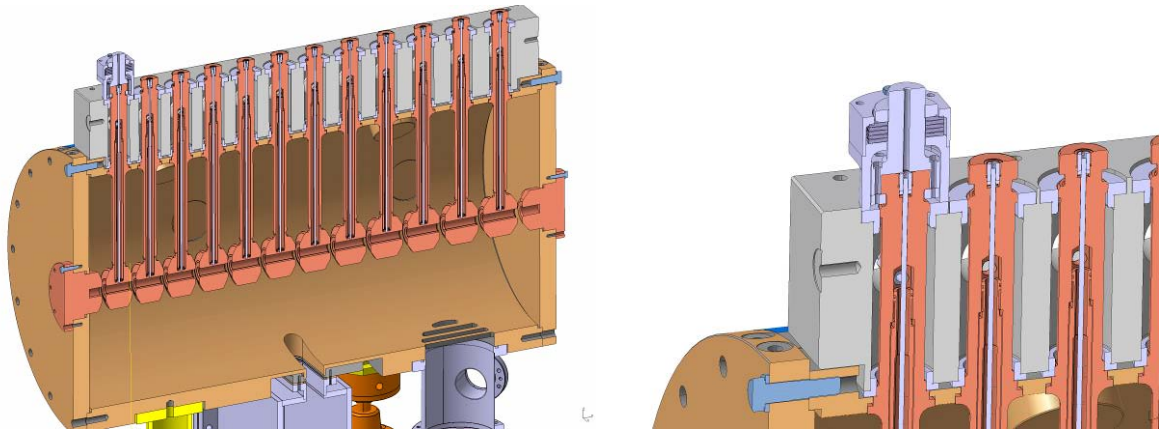


Figure 11: 3D view of the DTL prototype.

The cavities are made from 50 mm thick mild steel cylinders that provide the rigidity to achieve the required tolerances when placed on supports. The cavity is segmented into 2 sections in the first cavity, and 4 sections in the second and third cavity that are aligned with precisely machined rings after assembly of each section. Mild steel is the material of choice due to its thermal conductivity, mechanical strength, and comparably low price [4].

The steel cylinders of about 1.8 m length are precision machined in order to correctly position rectangular aluminium girders on top. The girders are pre-machined for each drift tube and stainless steel rings are inserted into the openings from above and below. The steel rings are re-machined for precise drift tube positioning.

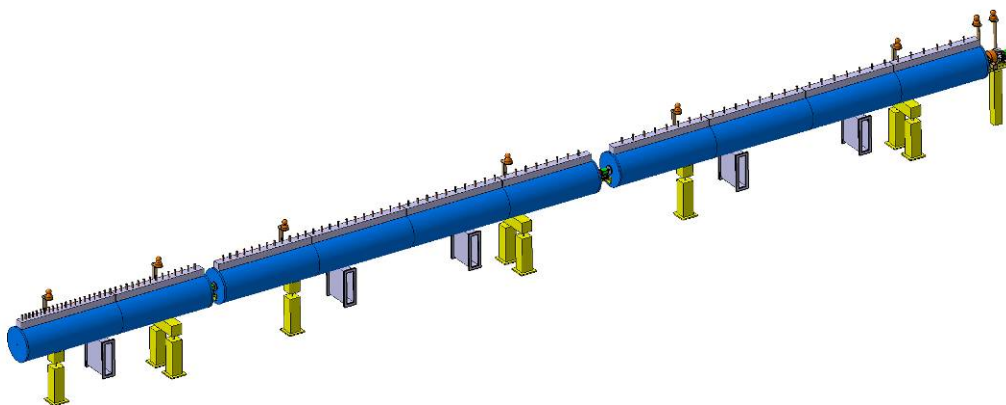


Figure 12: 3D view of the full DTL section.

Drift Tube Mount Assembly

The completed girder is placed on the steel cylinder and provides the reference for drift tube mounting (Fig. 13). The horizontal position of the drift tube is defined via the lever arm between upper and lower steel rings whereas the vertical position is given by the stop position on the lower ring.

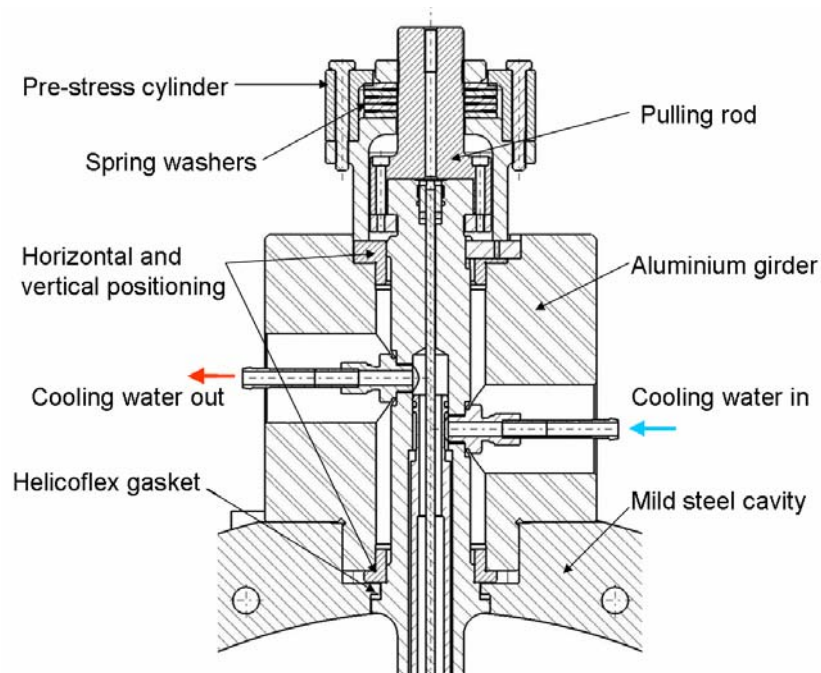


Figure 13: Drift tube mount assembly.

At the top, the copper drift tube is extended by a stainless steel pulling rod as the length of the drift tube shaft that can be installed in the cavity is limited by the diameter of the cavity. The Helicoflex[®] gasket rests on a stop on the drift tube and provides for vacuum tightness and RF continuity towards the copper plated mild steel cavity. Spring washers at the top of the drift tube provide the required force via a nut to compress the Helicoflex[®] gaskets.

For the installation of the spring washers a pre-compression socket is assembled in advance with the lower support socket. This pre-assembly is placed over the pulling rod and rests on the upper stainless steel ring. The nut is placed on the extension rod and just locked on the spring washers. The pre-compression cylinder is released in a way that the compression force is transferred uniformly to the drift tube through the nut and the extension rod.

Drift Tube Design

The drift tube design with PMQ for the Linac4 DTL follows the prototype study of the ISTC project 2888. The drift tube needs to be cooled in order to extract the heat from Ohmic losses on RF surfaces. The cooling circuit operates in a coaxial setup with ingoing water in the outer layer and outgoing water in the inner layer. Details are shown in figure 14 & 15.

The fact that the drift tube needs to be assembled including cooling circuits and PMQ to high precision requires a specific assembly procedure for all parts:

- Machining of drift tube parts with main references
- Assembly of cooling circuit in the drift tube core
- Assembly of drift tube with stem by e-beam welding
- Vacuum test of cooling circuit
- Final machining of magnet holder and references
- Insertion of the permanent magnet quadrupole (PMQ)
- Closure of drift tube by e-beam welding
- Metrology

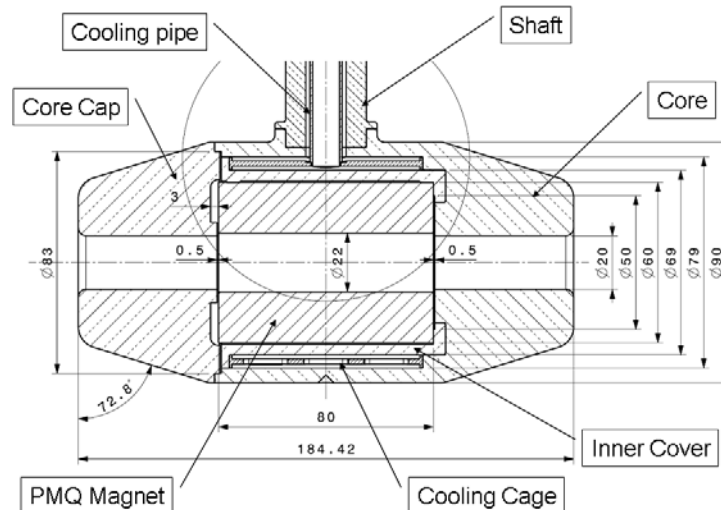


Figure 14: Drift tube core with PMQ.

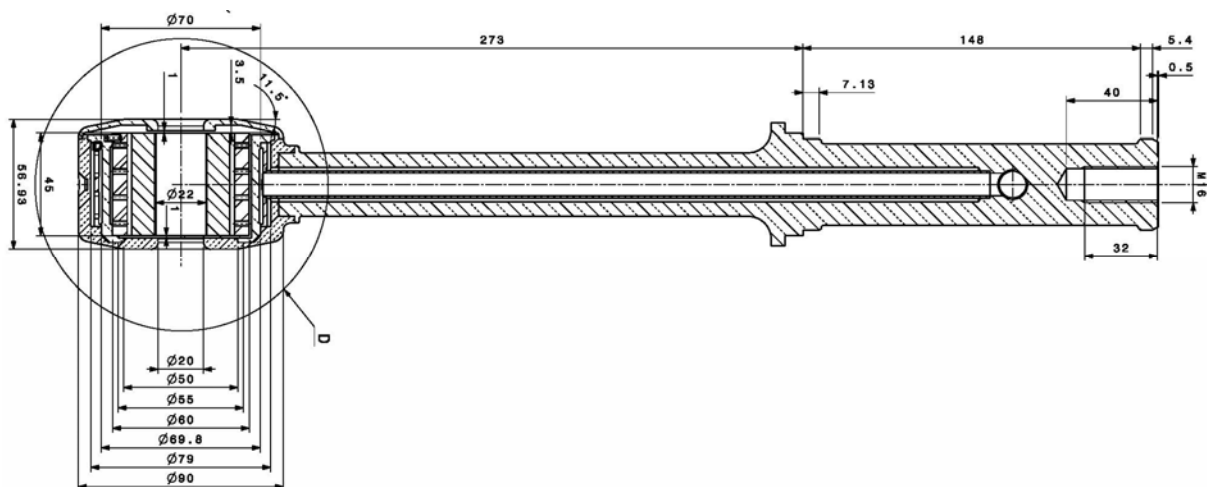


Figure 15: Drift tube with shaft.

Prototyping

In order to test the key technologies of the DTL manufacturing and assembly with respect to procedures, alignment precision, power loss, peak electric fields, tuning and stabilization as well as vacuum tightness, and in order to verify the correctness of the design, it was decided to build a prototype of about 1 m length (Fig. 11 and 16) and a pre-prototype of 320 mm length.

The DTL prototype structure consists of 13 cells (12 drift-tubes) of a final DTL cavity. It reuses the 300 kW power coupler of the CCDTL prototype design [3]. The pre-prototype consists in a mock-up of just two cells in order to test assembly procedures well before the final pieces would be available and to get a good idea on the requirements for the drift tube assembly.

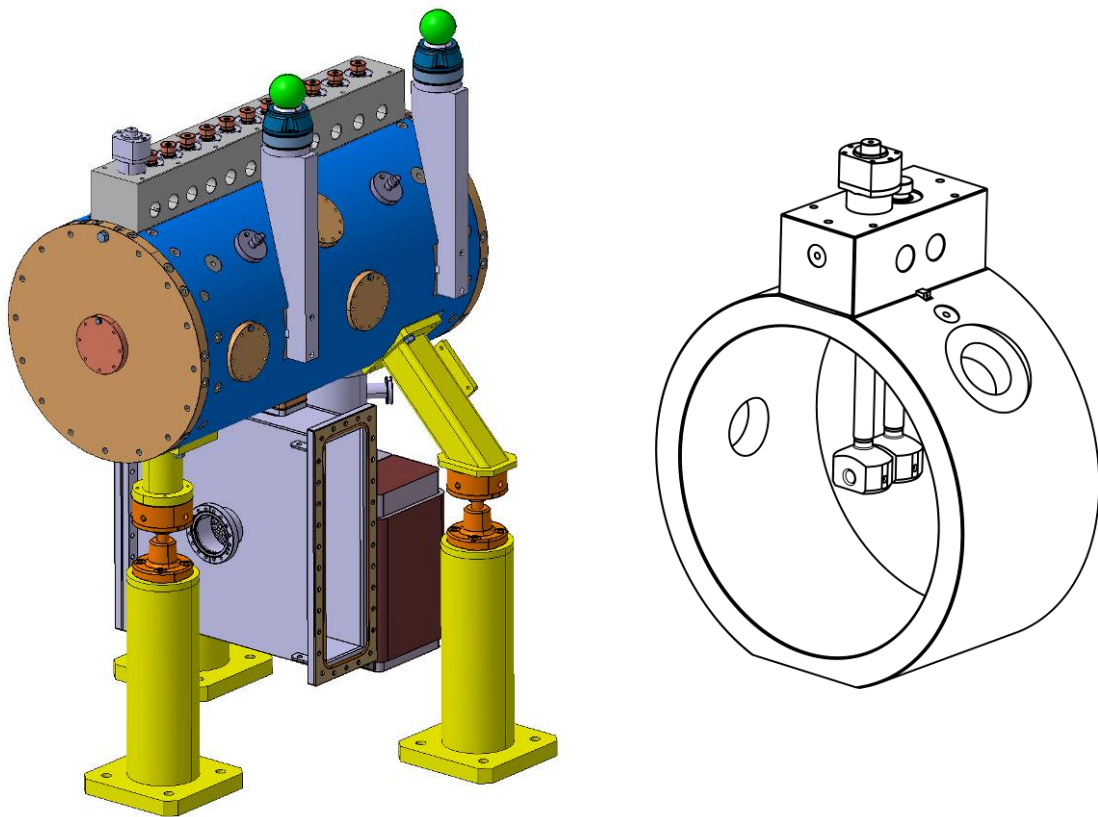


Figure 16: The DTL prototype with 12 drift tubes and the pre-prototype with 2 drift-tubes.

DTL pre-prototype

All major parts of the pre-prototype have been dimensionally checked. Results show minor deviations which are acceptable with respect to the purpose of procedure verification. The assembly of the drift tube cores with the drift tube stems by e-beam welding was tested and the two drift tubes show excellent results in two dimensions. The third dimension (longitudinal with respect to the beam direction) however shows deviations of up to 0.22 mm.

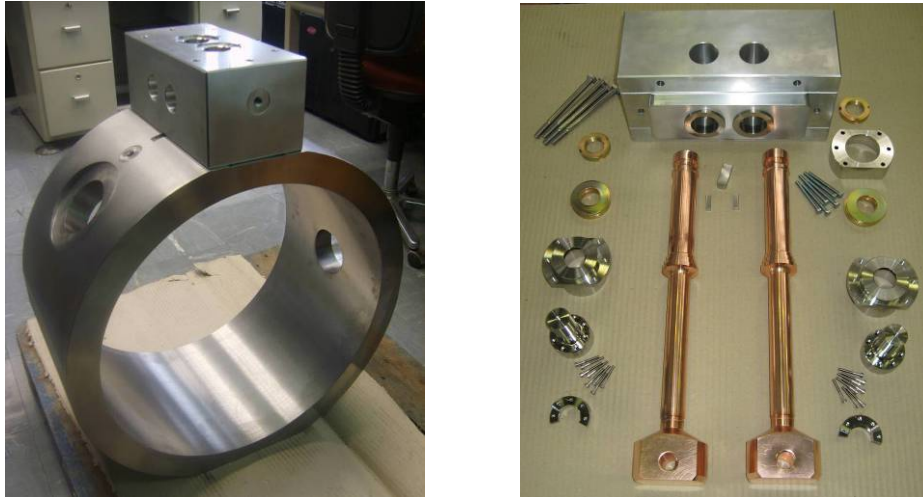


Figure 17: Completed parts of the pre-prototype structure.

The assembly of the two dummy drift tubes showed that the drift tube assembly procedure for the final drift tubes must be defined in detail and all parameters for weld connections must be found in advance in order to achieve the required tolerances. The mechanical assembly of the prototype turned out to be straightforward with the means that had been foreseen for the assembly. Minor improvements and further tooling could be prepared in order to further ease the assembly of the prototype.



Figure 18: The assembled pre-prototype structure.

The pre-prototype structure was measured using a laser tracker system and the drift tube positions were found to be in tolerances.

DTL Prototype

Following the delivery of the machining pieces of the DTL prototype produced by the Italian company CINEL and provided by INFN, Legnaro free of charge, the drift tube cores and stems, as well as the girder and the cavity have been dimensionally checked and have been found acceptable with respect to the required tolerances. After metrology, the cavity and end-covers then were copper plated at CERN.

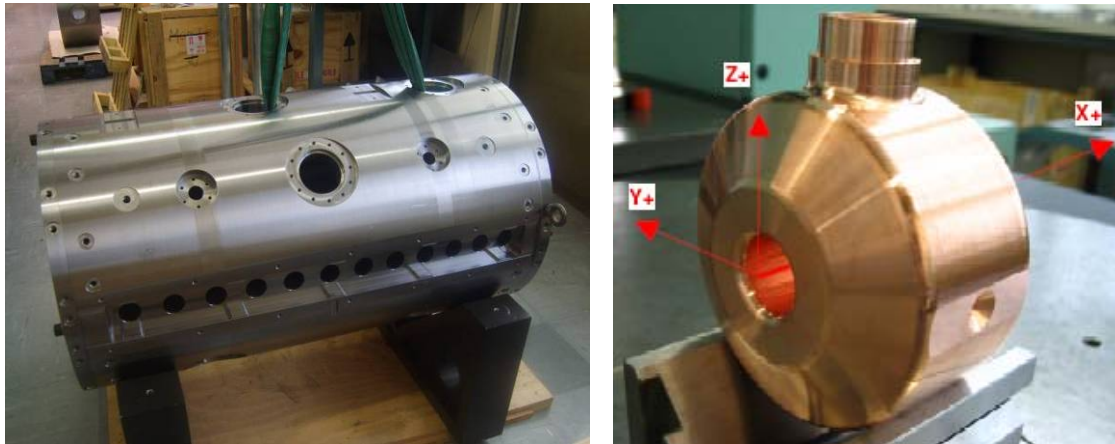


Figure 19: DTL prototype cavity and drift tube core after machining.

For the assembly of the prototype structure, the welding procedure for the drift tube to stem connection was further tested on samples. Based on the results of these tests the 12 prototype drift tubes were assembled and measured piece by piece in the metrology lab. Apart from 2 drift tubes where problems in welding caused major deviations, all drift tubes show consistent results (Table 4). Vertically, the systematic error stems from a contraction of the weld area and can be compensated by design. The horizontal drift tube position requires further improvement on final structures. Longitudinally, the error is less critical.

Metrology Drift Tube					
Center calculated					
No point	X (horiz)	Y (long)	Z (vert)	Y (yaw)	X (roll)
1	-0.037	0.001	0.053	-2.161E-04	-5.146E-05
2	-0.078	0.125	0.081	-1.029E-04	-1.081E-03
3	0.000	0.027	0.049	-3.809E-04	1.750E-04
4	-0.028	-0.018	0.060	-2.059E-04	-2.471E-04
5	-0.043	-0.016	0.054	-1.132E-04	-9.262E-04
6	-0.124	0.046	0.063	2.058E-04	-2.151E-03
7	-0.002	-0.026	0.072	1.956E-04	3.604E-04
8	-0.020	-0.010	0.059	-1.030E-05	2.677E-04
9	-0.055	-0.020	0.043	1.956E-04	-4.632E-04
10	-0.017	-0.019	0.065	-2.985E-04	2.573E-04
11	-0.027	-0.004	0.067	-2.265E-04	-4.530E-04
12	0.006	-0.014	0.067	-2.060E-04	2.162E-04
AVG	-0.035	0.006	0.061	-9.694E-05	-3.413E-04
STDEV	0.037	0.043	0.010	2.015E-04	7.437E-04
MID	-0.062	0.050	0.062	0.000	-0.001
MAXMIN/2	0.065	0.075	0.019	2.934E-04	1.256E-03
MAXABS	0.124	0.125	0.081	3.809E-04	2.151E-03

Table 4: DT metrology data after weld assembly

Mounting of drift tubes in the DTL cavity was straightforward and could be done within 2 days (Fig. 20). Following the assembly, the drift tube positions were measured by laser tracker and all were found to be within tolerances which are ± 0.1 mm and ± 3 mrad in all three dimensions (Table 5).

Survey						
Center calculated						
No point	X (horiz)	Y (long)	Z (vert)	Y (yaw)	Z (roll)	
1	0.015	0.000	-0.002	0.000E+00	-1.655E-04	
2	-0.035	0.142	0.016	1.407E-03	-1.200E-03	
3	0.041	0.063	-0.007	4.244E-04	6.210E-05	
4	-0.018	0.029	-0.003	1.283E-03	-4.037E-04	
5	0.008	0.001	-0.021	-1.604E-03	-6.621E-04	
6	-0.066	0.057	0.003	-8.483E-04	-2.472E-03	
7	0.050	0.042	0.016	5.487E-04	-8.283E-05	
8	0.042	0.075	0.005	-1.180E-03	1.553E-04	
9	-0.056	0.136	-0.025	5.074E-04	-7.145E-04	
10	0.026	0.108	0.033	-2.589E-04	1.118E-03	
11	-0.007	0.146	-0.008	5.488E-04	-6.006E-04	
12	-0.002	0.074	-0.007	-9.841E-04	1.968E-04	
AVG	0.000	0.073	0.000	-1.292E-05	-3.975E-04	
STDEV	0.038	0.052	0.016	9.717E-04	8.781E-04	
MID	-0.008	0.073	0.004	-9.806E-05	-6.770E-04	
MAXMIN/2	0.058	0.073	0.029	1.506E-03	1.795E-03	
MAXABS	0.066	0.146	0.033	1.604E-03	2.472E-03	

Table 5: Laser tracker measurements show all 12 drift tubes in tolerances.

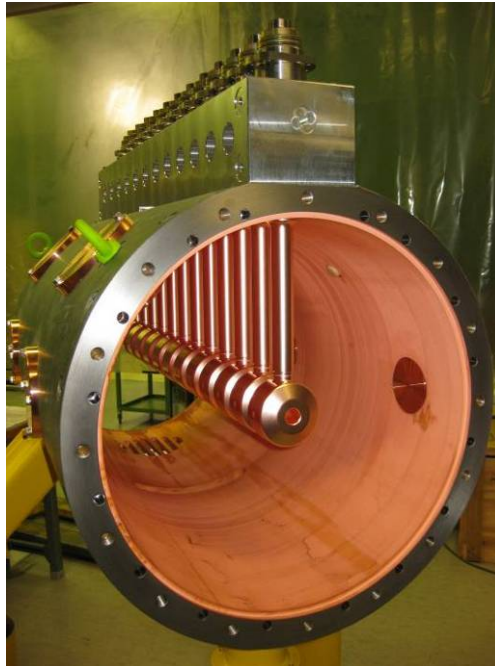


Figure 20: DTL prototype cavity assembled with 12 drift tubes

Following this nice result, the end covers and the wave-guide were mounted on the prototype cavity in order to prepare the cavity for RF measurements.

RF Measurement Results

The completed prototype cavity has undergone low power measurements so far. The results are consistent with the simulations of the prototype. A quality factor Q of 34190 (structure without post-couplers and shorted RF-port) was found which is about 80% of the simulated Q of 42670 from Superfish calculations. The losses are within the range of what is expected for such a structure in particular when it is short. The reduction in Q is due to an increase in surface resistance from roughness, tuners and RF contacts.

The resonance frequency with tuners fully inserted, without post-couplers and with a short-circuited RF-port iris was found to be 352.115 MHz compared to a simulated frequency of 352.343 MHz. The remaining difference can be attributed to the 2D approximation of tuners (~ 140 kHz according to 3D simulations), and machining errors on cavity and drift tube dimensions.

In order to properly stabilize the cavity with the system of post-couplers, coupling between the accelerating mode and the post-coupler mode has to be achieved. Figure 21 shows the resonant frequencies of the accelerating mode together with the resonance frequencies of the post-coupler mode in relation to the post-coupler length. At specific post-coupler lengths three of the four post-coupler modes are in confluence with the accelerating mode. The correct post-coupler length for operating the cavity is where the gap distance is below the PC-0 mode confluence point.

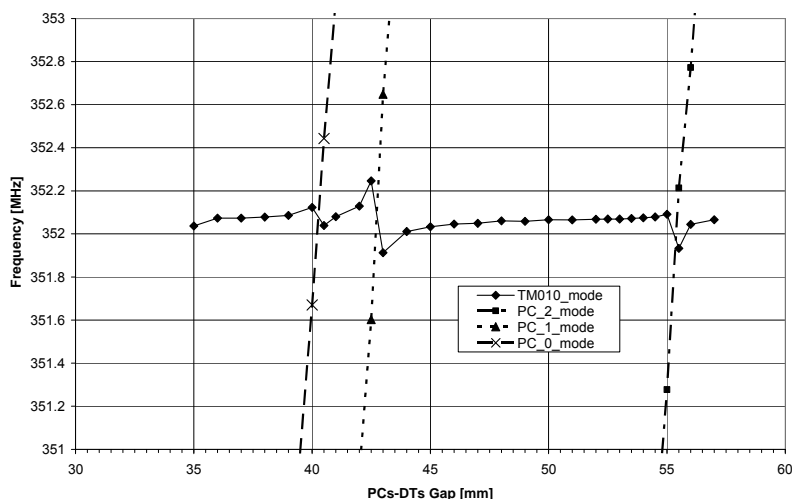


Figure 21: Mode frequencies for various post-coupler to drift-tube gaps

The exact post-coupler lengths have to be determined by bead pull measurements as shown in figure 22. Systematically tuned and detuned bead-pull measurements define the tilt-sensitivity that represents a measure for the stability of the cavity with respect to mechanical deformation due to local heating of the accelerating structures. [8]

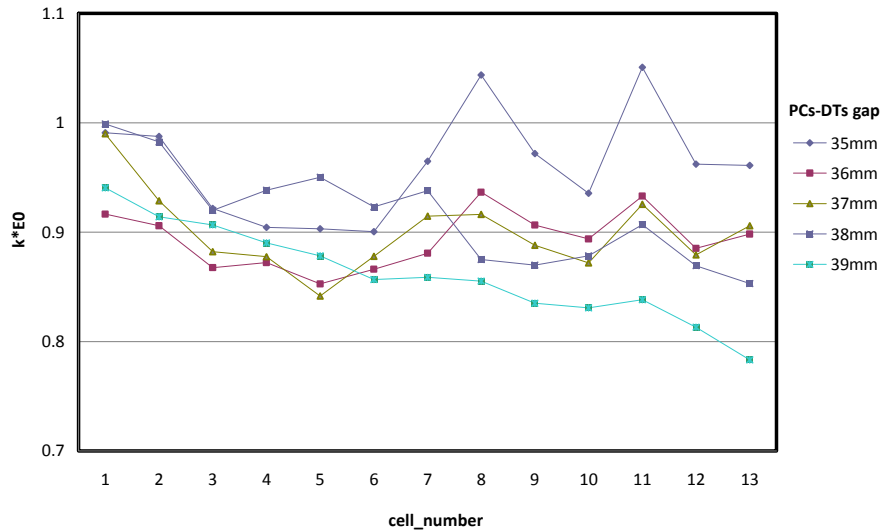


Figure 22: Bead pull measurements for various post-coupler to drift-tube gaps

In order to study the stabilization of the DTL cavities in more detail, a scaled tuning model has been manufactured from aluminium and brass as a Saudi-Arabian contribution (Fig. 23). The model has been tuned and stabilized as can be seen in the measurements.

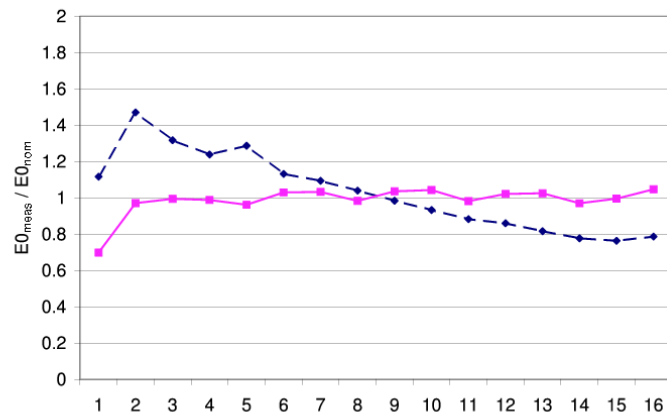
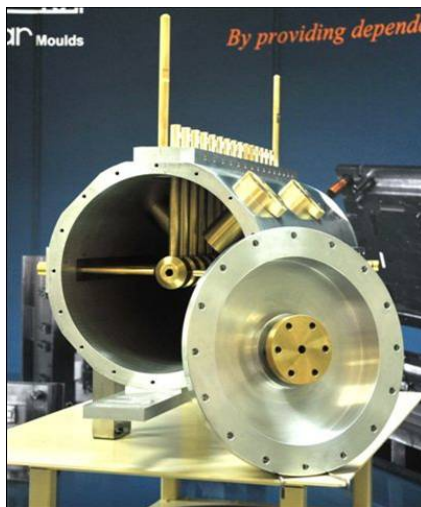


Figure 23: Tuning model and post-coupler stabilization.

Acknowledgements

We acknowledge the support of the European Community-Research Infrastructure Activity under the FP6 “Structuring the European Research Area” programme (CARE, contract number RII3-CT-2003-506395).

We are grateful for the support by Andrea Pisent with the INFN, Legnaro, for financing and Roberto Baruzzo with Strumenti Scientifici CINEL s.r.l. for manufacturing the machining parts of the prototype. We would like to particularly mention the tuning model designed by Nader Alharbi and built at the KACST, Riyadh, with financial support of Saudi Arabia. The design principle of the drift tube cooling circuit is an acknowledged outcome of studies within the ISTC project 2888.

The CERN work-shops and various groups provided manufacturing and testing support for the prototypes, and we would like to thank Jean-Pierre Brachet, Vladimir Bretin, Marco Buzio, Ahmed Cherif, Jacky Carosone, Monique Dupont, Gilles Favre, Jean-Marie Geisser, Alexandre Gerardin, Didier Glaude, Francesco Grespan, Mark Jones, Marina Malabaila, Sophie Meunier, Ricardo de Moraes Amaral, Eric Page, Marc Polini, Dominique Pognat, Christian Saint-Jal, Stefano Sgobba, Thierry Tardy, Marc Thiebert, Giovanna Vandoni, et al.

References

- [1] J. H. Billen, L. M. Young “Poisson Superfish”, LA-UR-96-1834, Los Alamos, 2002
- [2] D. Uriot, N. Pichoff, “GENDTL”, internal report CEA/DSM/DAPNIA/SEA/2000/46
- [3] G. De Michele et al., “CCDTL section for Linac4”, Tech. Rep. CARE-Report-08-021-HIPPI, CARE 2008.
- [4] J. Stovall, “Low and Medium Energy Beam Acceleration in High Intensity Linacs”, Proc. EPAC 2004, Lucerne, Switzerland, 2004, pp. 108-112.
- [5] A. M. Lombardi et al., “End-to-End Beam Dynamics for CERN LINAC4”, Tech. Rep. CERN-AB-2007-001 / CARE-Conf-06-039-HIPPI, CERN, Geneva, Aug 2006.
- [6] P. M. Lapostolle and A. L. Septier, Linear accelerators, North-Holland, Amsterdam, 1970.
- [7] A. Moretti et al., “Effects of high solenoidal magnetic fields on rf accelerating cavities”, Phys. Rev. ST Accel. Beams 8 (2005) 7, p. 072001.
- [8] N. Alharbi, F. Gerigk and M. Vretenar, “Field Stabilization with Post Couplers for DTL Tank1 of Linac4”, Tech. Rep. CARE-Note-2006-012-HIPPI, CARE, 2006.
- [9] P.-E. Bernaudin, “RF design of a DTL power coupler”, CARE/HIPPI Document-2005-002
- [10] E. Vernay, J.-M. De Conto, D. Bondoux, “Thermomechanical study of the HIPPI/LINAC4 DTL coupling port. Results for the ‘connecting guide’ part.”, CARE/HIPPI Document-2005-010
- [11] S. Ramberger et al., “Design and manufacturing of a DTL prototype power coupler”, Tech. Rep. CARE-Report-08-009-HIPPI; CARE 2008.

Appendix

Tank by tank and cell by cell data of a self-consistent RF-design for the CERN Linac4 DTL

Tank1:

Cell	L_{cell}	g/l	α_f	Kilp	β_{in}	T	$Z_s \text{TT}$	E_{stored}	P_{Cu}	φ_s	E_{Gain}	E_{Out}	L_{tot}
1	6.87	0.189	4.12	1.20	0.0797	0.75	14.70	0.220	26.76	-30.00	0.142	3.14	6.87
2	7.03	0.190	4.26	1.20	0.0816	0.75	31.57	0.226	12.98	-29.50	0.148	3.29	13.89
3	7.19	0.191	4.48	1.20	0.0835	0.76	32.34	0.231	13.18	-29.00	0.153	3.44	21.08
4	7.35	0.192	4.79	1.20	0.0854	0.77	33.10	0.236	13.39	-28.50	0.159	3.60	28.43
5	7.52	0.192	5.10	1.20	0.0873	0.77	33.84	0.241	13.60	-28.00	0.164	3.77	35.95
6	7.69	0.183	8.64	1.25	0.0893	0.78	35.12	0.246	13.80	-27.50	0.171	3.94	43.64
7	7.86	0.175	12.18	1.30	0.0913	0.79	36.33	0.251	13.99	-27.00	0.178	4.12	51.50
8	8.03	0.167	16.24	1.35	0.0933	0.80	37.55	0.256	14.18	-26.50	0.185	4.30	59.53
9	8.21	0.161	20.30	1.40	0.0954	0.81	38.69	0.261	14.38	-26.00	0.192	4.49	67.74
10	8.39	0.155	24.82	1.45	0.0975	0.82	39.83	0.266	14.56	-25.50	0.199	4.69	76.14
11	8.57	0.150	29.74	1.50	0.0996	0.83	40.95	0.271	14.74	-25.00	0.206	4.90	84.71
12	8.76	0.144	35.98	1.55	0.1017	0.84	42.20	0.275	14.88	-24.50	0.213	5.11	93.47
13	8.94	0.140	42.63	1.60	0.1039	0.84	43.33	0.280	15.04	-24.00	0.221	5.33	102.41
14	9.13	0.141	44.19	1.59	0.1061	0.85	44.12	0.285	15.22	-23.50	0.227	5.56	111.54
15	9.32	0.140	47.22	1.60	0.1083	0.85	44.96	0.290	15.41	-23.00	0.234	5.79	120.87
16	9.51	0.141	48.77	1.59	0.1105	0.86	45.65	0.296	15.62	-22.50	0.241	6.03	130.38
17	9.71	0.141	52.47	1.60	0.1128	0.86	46.52	0.301	15.79	-22.00	0.248	6.28	140.09
18	9.90	0.141	54.98	1.60	0.1151	0.86	47.16	0.307	16.02	-21.50	0.254	6.54	149.99
19	10.10	0.142	56.55	1.59	0.1174	0.87	47.78	0.312	16.23	-21.00	0.261	6.80	160.09
20	10.29	0.143	59.40	1.60	0.1196	0.87	48.53	0.317	16.41	-20.50	0.268	7.06	170.38
21	10.48	0.144	60.00	1.58	0.1220	0.87	49.01	0.323	16.64	-20.00	0.275	7.34	180.85
22	10.67	0.146	60.80	1.57	0.1243	0.87	49.50	0.329	16.87	-20.00	0.281	7.62	191.53
23	10.87	0.148	61.50	1.55	0.1266	0.88	49.96	0.335	17.11	-20.00	0.286	7.91	202.40
24	11.07	0.149	62.10	1.55	0.1289	0.88	50.34	0.341	17.37	-20.00	0.292	8.20	213.47
25	11.27	0.151	62.80	1.53	0.1313	0.88	50.75	0.347	17.61	-20.00	0.298	8.50	224.74
26	11.47	0.153	63.40	1.52	0.1336	0.88	51.13	0.353	17.86	-20.00	0.304	8.80	236.21
27	11.67	0.154	64.00	1.50	0.1359	0.88	51.49	0.359	18.10	-20.00	0.310	9.11	247.87
28	11.87	0.156	64.50	1.49	0.1383	0.88	51.82	0.365	18.35	-20.00	0.316	9.43	259.74
29	12.07	0.158	65.10	1.48	0.1406	0.89	52.13	0.371	18.61	-20.00	0.321	9.75	271.80
30	12.26	0.159	65.60	1.46	0.1430	0.89	52.42	0.377	18.86	-20.00	0.327	10.07	284.07
31	12.46	0.161	66.00	1.45	0.1453	0.89	52.69	0.384	19.12	-20.00	0.333	10.41	296.53
32	12.66	0.163	66.50	1.44	0.1476	0.89	52.95	0.390	19.37	-20.00	0.339	10.75	309.20
33	12.86	0.165	67.00	1.43	0.1500	0.89	53.18	0.396	19.63	-20.00	0.344	11.09	322.06
34	13.06	0.167	67.40	1.42	0.1523	0.89	53.40	0.402	19.89	-20.00	0.350	11.44	335.12
35	13.26	0.168	67.80	1.40	0.1547	0.89	53.61	0.408	20.14	-20.00	0.356	11.80	348.38
36	13.46	0.170	68.20	1.39	0.1570	0.89	53.84	0.414	20.39	-20.00	0.361	12.16	361.84

Length in cm, Phase in deg, Power in kW, Energy in MeV, Stored Energy in Joule

Tank 2:

Cell	L_{cell}	g/l	α_f	Kilp	β_{in}	T	Z_{sTT}	E_{stored}	P_{Cu}	ϕ_s	E_{Gain}	E_{Out}	L_{tot}
1	13.66	0.172	68.70	1.39	0.1593	0.89	32.62	0.420	34.19	-20.00	0.367	12.52	13.66
2	13.86	0.174	69.10	1.38	0.1617	0.89	54.15	0.426	20.92	-20.00	0.372	12.90	27.52
3	14.06	0.176	69.40	1.38	0.1640	0.89	54.29	0.432	21.18	-20.00	0.378	13.27	41.58
4	14.26	0.178	69.70	1.37	0.1664	0.89	54.42	0.438	21.44	-20.00	0.383	13.66	55.83
5	14.46	0.179	70.10	1.37	0.1687	0.89	54.54	0.444	21.71	-20.00	0.389	14.05	70.29
6	14.65	0.181	70.40	1.36	0.1710	0.89	54.64	0.450	21.97	-20.00	0.394	14.44	84.94
7	14.85	0.183	70.70	1.36	0.1734	0.89	54.73	0.456	22.23	-20.00	0.399	14.84	99.80
8	15.05	0.185	70.90	1.36	0.1757	0.89	54.80	0.462	22.50	-20.00	0.405	15.24	114.85
9	15.25	0.187	71.20	1.35	0.1780	0.89	54.86	0.469	22.77	-20.00	0.410	15.65	130.09
10	15.44	0.189	71.50	1.35	0.1803	0.89	54.92	0.475	23.04	-20.00	0.415	16.07	145.54
11	15.64	0.191	71.70	1.35	0.1826	0.89	54.95	0.481	23.31	-20.00	0.421	16.49	161.18
12	15.84	0.193	72.00	1.34	0.1850	0.89	55.00	0.487	23.57	-20.00	0.426	16.92	177.02
13	16.04	0.195	72.20	1.34	0.1873	0.89	55.01	0.493	23.85	-20.00	0.431	17.35	193.05
14	16.23	0.197	72.40	1.33	0.1896	0.89	55.01	0.499	24.12	-20.00	0.436	17.78	209.28
15	16.43	0.199	72.60	1.33	0.1919	0.89	55.01	0.505	24.39	-20.00	0.441	18.22	225.71
16	16.62	0.201	72.90	1.33	0.1942	0.89	55.02	0.511	24.66	-20.00	0.446	18.67	242.33
17	16.82	0.203	73.10	1.32	0.1965	0.89	55.00	0.517	24.93	-20.00	0.451	19.12	259.15
18	17.01	0.204	73.30	1.32	0.1988	0.89	54.97	0.523	25.20	-20.00	0.456	19.58	276.16
19	17.21	0.206	73.40	1.32	0.2010	0.89	54.92	0.529	25.48	-20.00	0.461	20.04	293.37
20	17.40	0.208	73.60	1.32	0.2033	0.89	54.88	0.535	25.75	-20.00	0.466	20.51	310.77
21	17.59	0.210	73.80	1.31	0.2056	0.89	54.83	0.541	26.03	-20.00	0.471	20.98	328.37
22	17.79	0.212	74.00	1.31	0.2079	0.89	54.78	0.547	26.30	-20.00	0.476	21.45	346.15
23	17.98	0.214	74.20	1.31	0.2101	0.89	54.71	0.553	26.58	-20.00	0.480	21.93	364.13
24	18.17	0.216	74.30	1.30	0.2124	0.89	54.63	0.559	26.85	-20.00	0.485	22.42	382.31
25	18.36	0.218	74.50	1.30	0.2147	0.89	54.56	0.565	27.13	-20.00	0.490	22.91	400.67
26	18.56	0.220	74.60	1.30	0.2169	0.89	54.46	0.571	27.41	-20.00	0.494	23.40	419.22
27	18.75	0.222	74.80	1.30	0.2191	0.89	54.37	0.577	27.68	-20.00	0.499	23.90	437.97
28	18.94	0.224	74.90	1.30	0.2214	0.88	54.26	0.583	27.96	-20.00	0.504	24.40	456.91
29	19.13	0.226	75.10	1.29	0.2236	0.88	54.16	0.588	28.23	-20.00	0.508	24.91	476.03
30	19.32	0.228	75.20	1.29	0.2258	0.88	54.04	0.594	28.51	-20.00	0.513	25.43	495.35
31	19.50	0.230	75.30	1.29	0.2281	0.88	53.92	0.600	28.79	-20.00	0.517	25.94	514.85
32	19.69	0.232	75.50	1.29	0.2303	0.88	53.81	0.606	29.06	-20.00	0.521	26.46	534.54
33	19.88	0.234	75.60	1.29	0.2325	0.88	53.67	0.612	29.34	-20.00	0.526	26.99	554.42
34	20.07	0.236	75.70	1.29	0.2347	0.88	53.53	0.618	29.62	-20.00	0.530	27.52	574.49
35	20.25	0.238	75.80	1.28	0.2369	0.88	53.39	0.624	29.90	-20.00	0.534	28.05	594.75
36	20.44	0.240	75.90	1.28	0.2391	0.88	53.24	0.630	30.18	-20.00	0.538	28.59	615.19
37	20.63	0.242	76.00	1.28	0.2413	0.87	53.09	0.635	30.45	-20.00	0.543	29.13	635.81
38	20.81	0.243	76.20	1.28	0.2434	0.87	52.95	0.641	30.72	-20.00	0.547	29.68	656.62
39	20.99	0.245	76.30	1.28	0.2456	0.87	52.79	0.647	31.00	-20.00	0.551	30.23	677.62
40	21.18	0.247	76.40	1.28	0.2478	0.87	52.63	0.653	31.28	-20.00	0.555	30.79	698.80
41	21.36	0.249	76.50	1.28	0.2499	0.87	52.46	0.658	31.56	-20.00	0.559	31.35	720.16
42	21.54	0.251	76.60	1.28	0.2521	0.87	36.01	0.664	46.22	-20.00	0.563	31.91	741.70

Length in cm, Phase in deg, Power in kW, Energy in MeV, Stored Energy in Joule

Tank 3:

Cell	L_{cell}	g/l	α_f	Kilp	β_{in}	T	Z_{sTT}	E_{stored}	P_{Cu}	ϕ_s	E_{Gain}	E_{Out}	L_{tot}
1	21.73	0.253	76.70	1.27	0.2542	0.87	35.97	0.670	46.52	-20.00	0.567	32.47	763.43
2	21.91	0.255	76.80	1.27	0.2564	0.87	51.94	0.676	32.39	-20.00	0.570	33.05	785.34
3	22.09	0.257	76.80	1.27	0.2585	0.86	51.74	0.681	32.68	-20.00	0.574	33.62	807.43
4	22.27	0.259	76.90	1.27	0.2606	0.86	51.55	0.687	32.95	-20.00	0.578	34.20	829.70
5	22.45	0.261	77.00	1.27	0.2627	0.86	51.37	0.693	33.23	-20.00	0.582	34.78	852.14
6	22.63	0.262	77.10	1.27	0.2648	0.86	51.18	0.698	33.50	-20.00	0.585	35.36	874.77
7	22.81	0.264	77.20	1.27	0.2669	0.86	50.99	0.704	33.78	-20.00	0.589	35.95	897.58
8	22.98	0.266	77.30	1.27	0.2690	0.86	50.80	0.710	34.05	-20.00	0.592	36.55	920.56
9	23.16	0.268	77.30	1.27	0.2711	0.86	50.58	0.715	34.34	-20.00	0.596	37.14	943.72
10	23.34	0.270	77.40	1.27	0.2732	0.85	50.39	0.721	34.61	-20.00	0.599	37.74	967.06
11	23.51	0.272	77.50	1.27	0.2753	0.85	50.19	0.726	34.89	-20.00	0.603	38.34	990.58
12	23.69	0.274	77.60	1.27	0.2773	0.85	49.99	0.732	35.16	-20.00	0.606	38.95	1014.26
13	23.86	0.275	77.60	1.27	0.2794	0.85	49.76	0.738	35.44	-20.00	0.610	39.56	1038.13
14	24.04	0.277	77.70	1.27	0.2814	0.85	49.56	0.743	35.72	-20.00	0.613	40.17	1062.17
15	24.21	0.279	77.80	1.26	0.2835	0.85	49.35	0.748	35.99	-20.00	0.616	40.79	1086.38
16	24.38	0.281	77.80	1.26	0.2855	0.84	49.13	0.754	36.27	-20.00	0.619	41.41	1110.76
17	24.55	0.283	77.90	1.26	0.2875	0.84	48.92	0.760	36.54	-20.00	0.623	42.03	1135.31
18	24.73	0.284	78.00	1.26	0.2895	0.84	48.71	0.765	36.81	-20.00	0.626	42.66	1160.04
19	24.90	0.286	78.00	1.26	0.2915	0.84	48.48	0.771	37.09	-20.00	0.629	43.29	1184.94
20	25.07	0.288	78.10	1.26	0.2935	0.84	48.26	0.776	37.36	-20.00	0.632	43.92	1210.00
21	25.24	0.290	78.10	1.26	0.2955	0.84	48.03	0.781	37.64	-20.00	0.635	44.55	1235.24
22	25.40	0.291	78.20	1.26	0.2975	0.83	47.81	0.787	37.91	-20.00	0.638	45.19	1260.64
23	25.57	0.293	78.30	1.26	0.2995	0.83	47.60	0.792	38.18	-20.00	0.641	45.83	1286.22
24	25.74	0.295	78.30	1.26	0.3015	0.83	47.36	0.798	38.46	-20.00	0.643	46.47	1311.96
25	25.91	0.297	78.40	1.26	0.3034	0.83	47.14	0.803	38.72	-20.00	0.646	47.12	1337.86
26	26.07	0.298	78.40	1.26	0.3054	0.83	46.91	0.808	39.01	-20.00	0.649	47.77	1363.93
27	26.24	0.300	78.50	1.26	0.3073	0.83	46.69	0.813	39.27	-20.00	0.652	48.42	1390.17
28	26.40	0.302	78.50	1.26	0.3093	0.82	46.45	0.819	39.55	-20.00	0.654	49.07	1416.57
29	26.57	0.303	78.60	1.26	0.3112	0.82	46.23	0.824	39.81	-20.00	0.657	49.73	1443.14
30	26.73	0.305	78.60	1.26	0.3131	0.82	33.28	0.829	55.40	-20.00	0.660	50.39	1469.87

Length in cm, Phase in deg, Power in kW, Energy in MeV, Stored Energy in Joule

Summary by tank:

	Kilp	T_{avg}	E_{stored}	P_{Cu}	P_{beam}	P_{tot}	Effic.	E_{avg}	E_{gain}	Len	$Z_{\text{sTT}_{\text{av}}}$
Tank 1	1.60	0.85	11.043	588.87	360.60	949.47	0.380	0.258	9.015	361.84	45.24
Tank 2	1.39	0.89	22.817	1127.99	790.04	1918.03	0.412	0.470	19.751	741.70	53.29
Tank 3	1.27	0.84	22.521	1113.27	739.32	1852.60	0.399	0.616	18.483	728.17	48.11

Power values are scaled up by 0.8, to account for additional losses with respect to simulations (e.g. post-couplers, tuners, RF port, RF contacts and surface roughness). Losses from stems are included in each cell, losses from end-walls are included in the first and last cell. ZTT values are scaled consistently with 0.8.